

Introduction

Toward CMIP6, we have developed a new version of earth system model MRI-ESM2. From previous version models (MRI-CGCM3/MRI-ESM1), we performed many improvements such as increase of resolution, refined treatments of cloud microphysics and aerosol, and etc. We performed CMIP6 setting historical experiment as a trial, and introduce the results of general performance and those focused on middle atmosphere.

Summary

- Realistic multi-decadal variation in global mean surface air temperature is simulated, and Equilibrium Climate Sensitivity (ECS) increases from previous version (2.6 K → 3.0 K).
- Cloud bias and radiative bias related to cloud are largely reduced.
- ENSO and related atmospheric patterns are realistic, and sea ice expression in NH improved.
- Realistic Quasi-Biennial Oscillation (QBO) is simulated.
- Temperature response to solar cycle is improved.
- Frequency of Stratospheric Sudden Warming (SSW) is improved.
- Ozone reduction related to Energetic Particle Precipitation (EPP) such as Halloween event in 2003 is realistically expressed.

Global mean surface air temperature

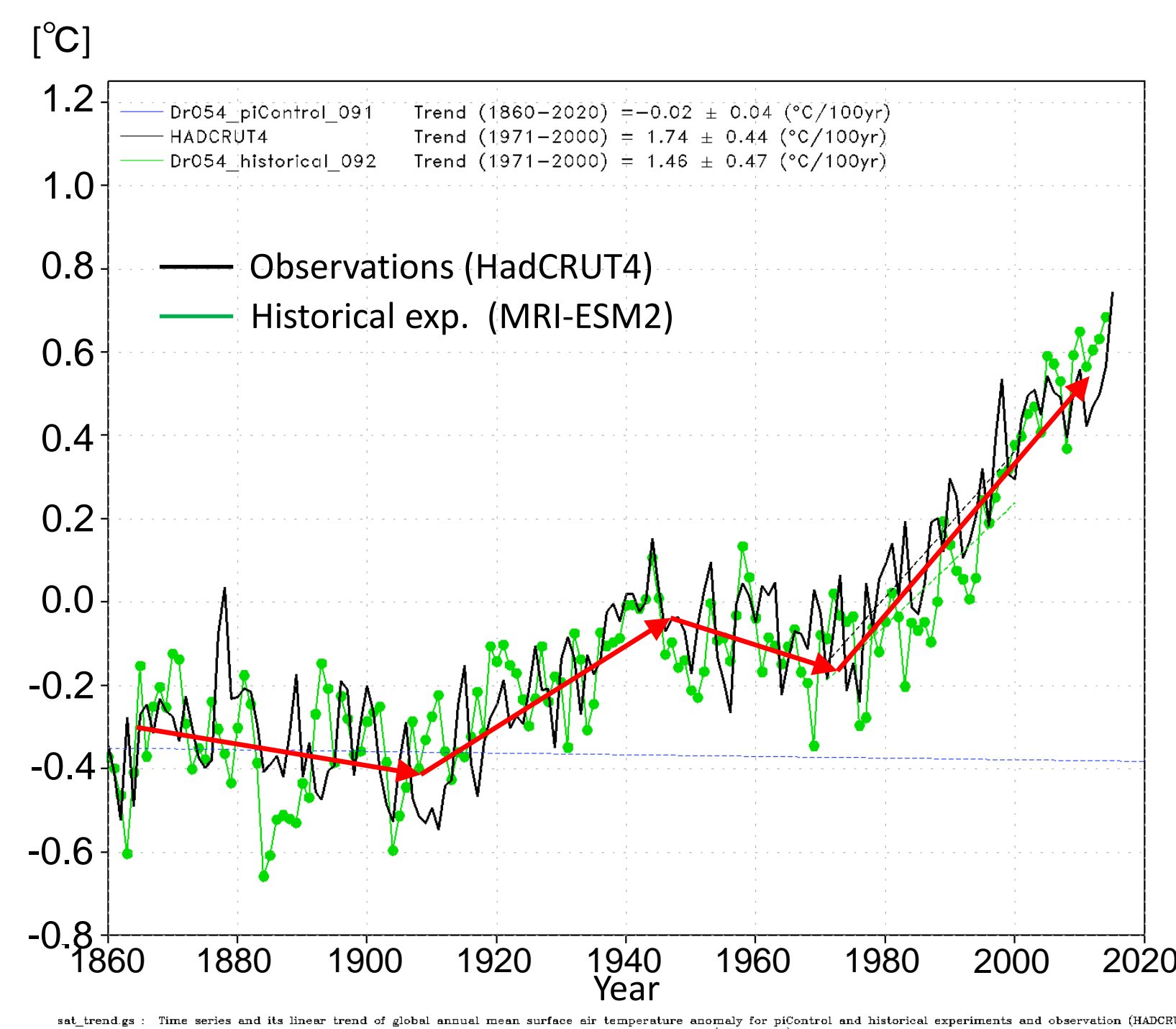


Fig. 2. Temporal evolution of global mean surface air temperature anomaly in (black) HadCRUT4 and (green) historical exp. of MRI-ESM2. The anomalies are adjusted to the base period (1861-1930) mean.

- MRI-ESM2 simulates realistic multi-decadal surface temperature variations!
- Equilibrium Climate Sensitivity is estimated by about 3.0 K* (MRI-CGCM3: 2.6 K).

*Result of slightly old model version

Bias of annual mean total cloud (historical, 1986-2005)

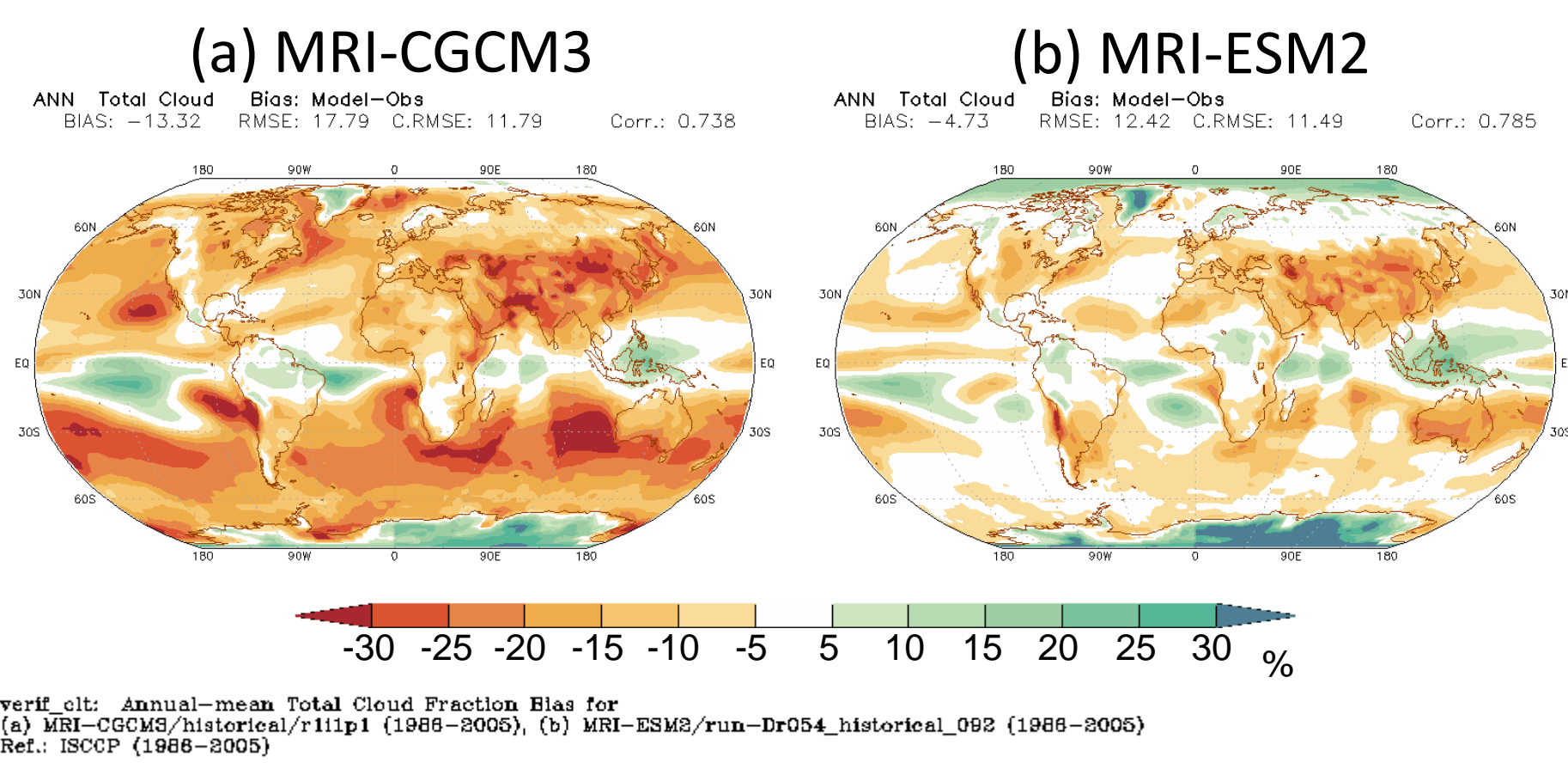


Fig. 3. Bias of annual mean total cloud fraction in (a) MRI-CGCM3 and (b) MRI-ESM2 averaged for 1986-2005. The biases are constructed from difference between model results and ISCCP.

- Bias reduces globally
- Improvement appears especially in the Southern Ocean and off the coast of Peru.
- Improvement of cloud contributes to radiative bias reduction.

Expression of ENSO

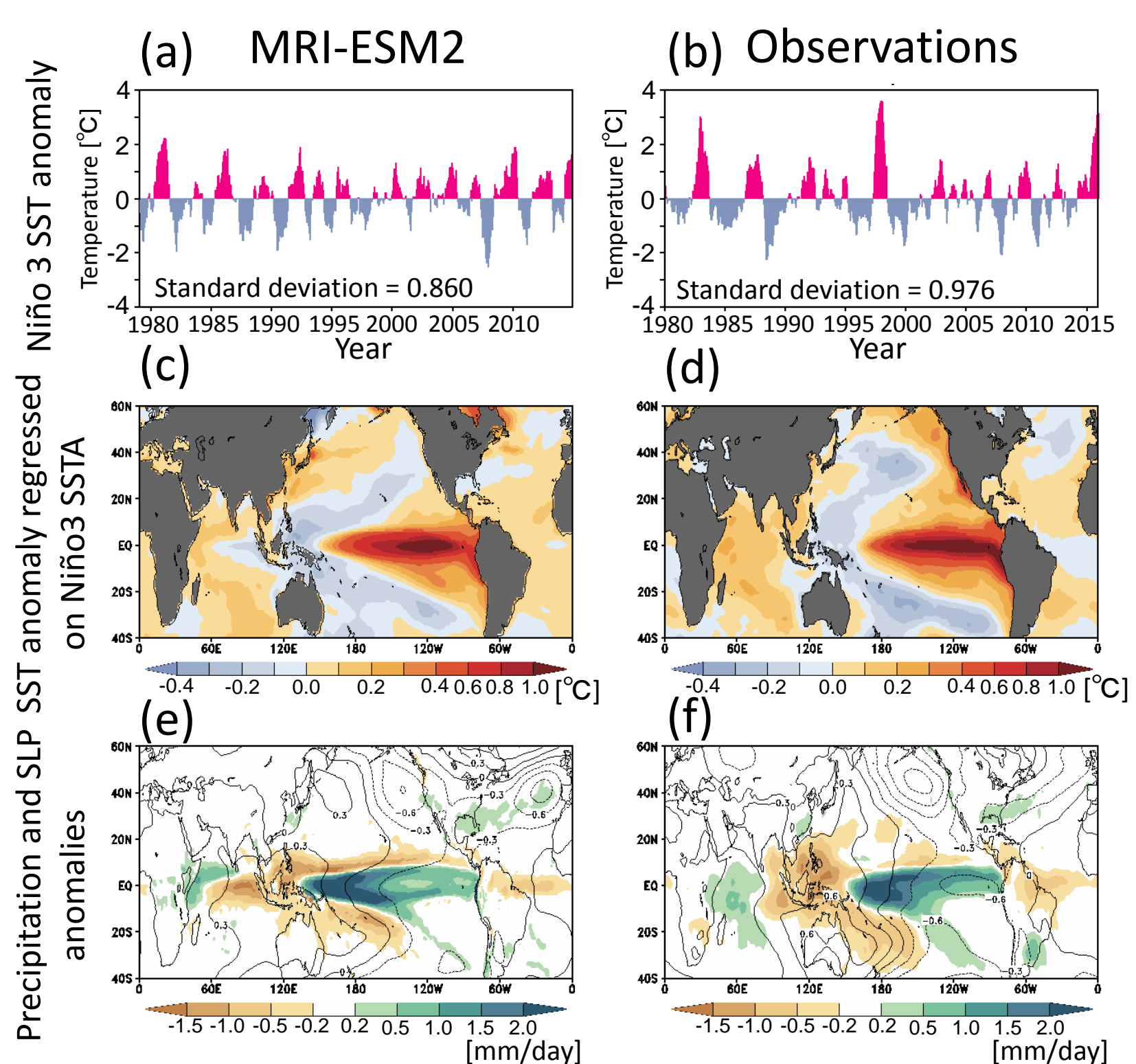


Fig. 4. (a,b) Time series of Niño3 SST anomaly, (c,d) SST anomaly regressed on Niño3 SST, and (e,f) precipitation and SLP anomalies regressed on Niño3 SST in (a,c,e) MRI-ESM2 and (b,d,f) observations.

- Variability of Niño3 SST is expressed realistic.
- Regressed spatial patterns of SST, precipitation, and SLP are resembles to observations.

Expression of sea ice

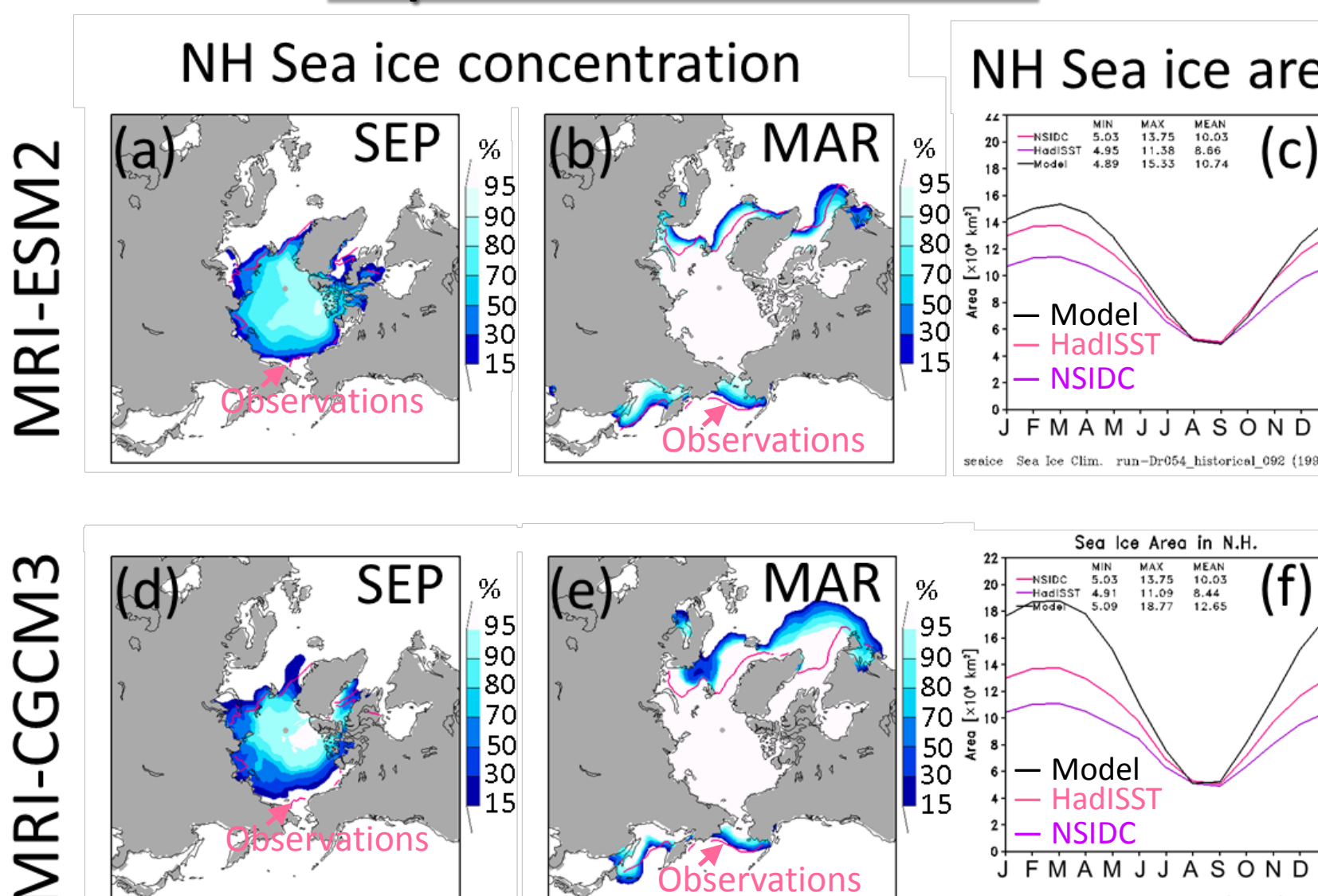


Fig. 5. Sea ice concentration simulated in MRI-ESM2 in Northern Hemisphere in (a) September and (b) March. (c) Seasonal variation of sea ice area in MRI-ESM2 accumulated over Northern Hemisphere. The calculation period is 1990-1995. (d-f) Same as (a-c) but for MRI-CGCM3 (old model version). Red and purple lines indicate observations.

- Distribution of sea ice concentration is improved especially in the Labrador Sea and Barents Sea.
- Excessive sea ice area in boreal winter is reduced.

Comparison of model structure between CMIP5 and CMIP6

MODEL	CMIP5	CMIP6
Atmosphere	MRI-ESM1/MRI-CGCM3	MRI-ESM2
Version	MRI-AGCM3.3	MRI-AGCM3.5
H. Resolution	T159 (~120km)	Same as CMIP5
V. Resolution	L48 (top:~0.01hPa)	L80 (top:~0.01hPa)
Ocean/Sea ice	MRI.COM-3	MRI.COM-4.4
Version	MRI.COM-3	MRI.COM-4.4
H. Resolution	1° (Lon) × 0.5° (Lat)	1° (Lon) × 0.5° (Lat, 0.3° in 10S-10N)
V. Resolution	L51	L60+BBL
Aerosol	MASINGAR mk2	MASINGAR mk2 rev.4
Version	MASINGAR mk2	MASINGAR mk2 rev.4
H. Resolution	T195 (~180km)	Same as CMIP5
V. Resolution	L48 (~0.01hPa)	L80 (~0.01hPa)
Atmospheric Chemistry	MRI-CCM2	MRI-CCM2.2
Version	MRI-CCM2	MRI-CCM2.2
H. Resolution	T42 (~280km)	Same as CMIP5
V. Resolution	L48 (~0.01hPa)	L80 (~0.01hPa)

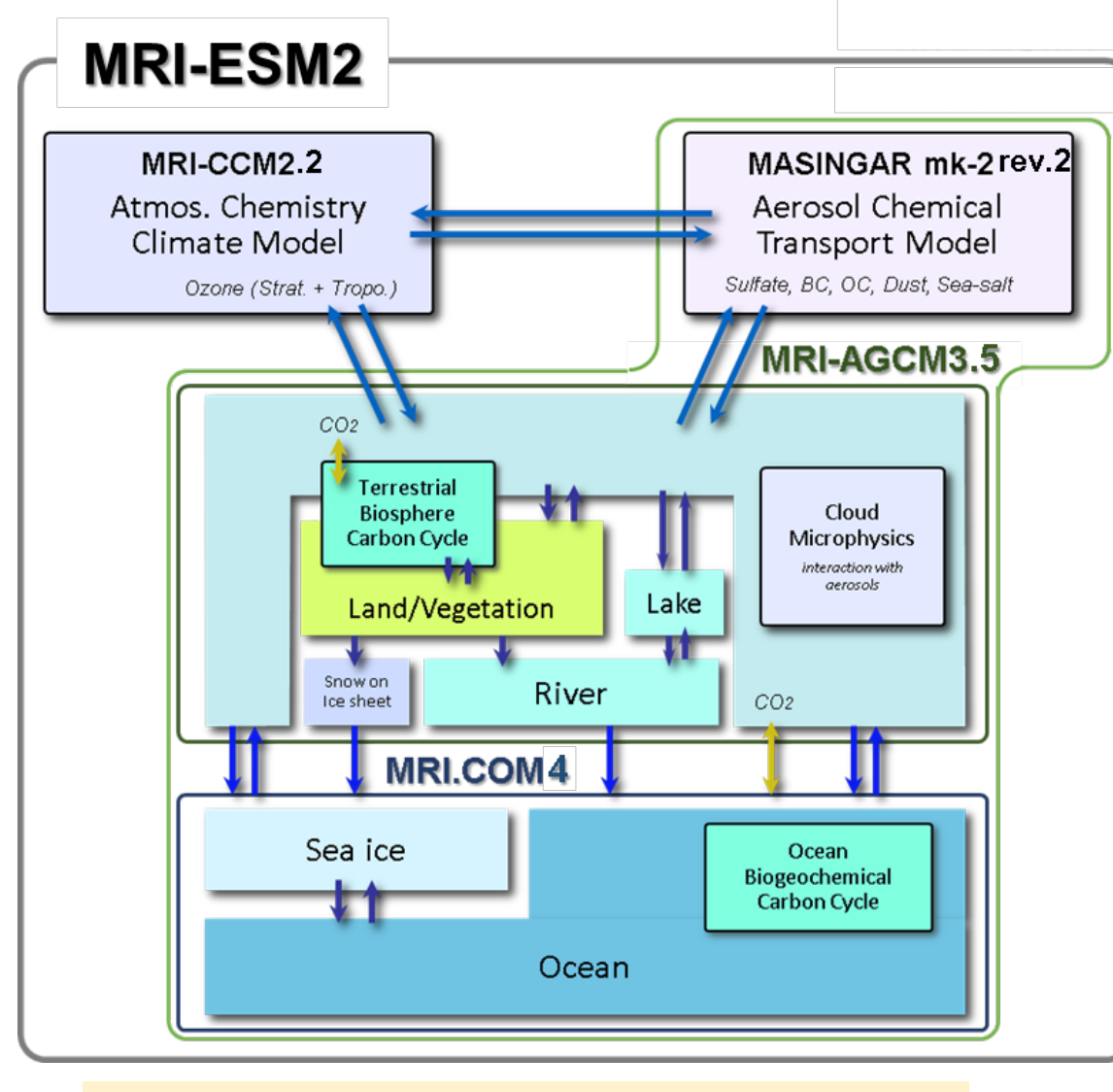


Fig. 1. Schematics of MRI-ESM2

- Increase of vertical resolution
- Many processes are refined in each model

Reproducibility of Quasi-Biennial-Oscillation

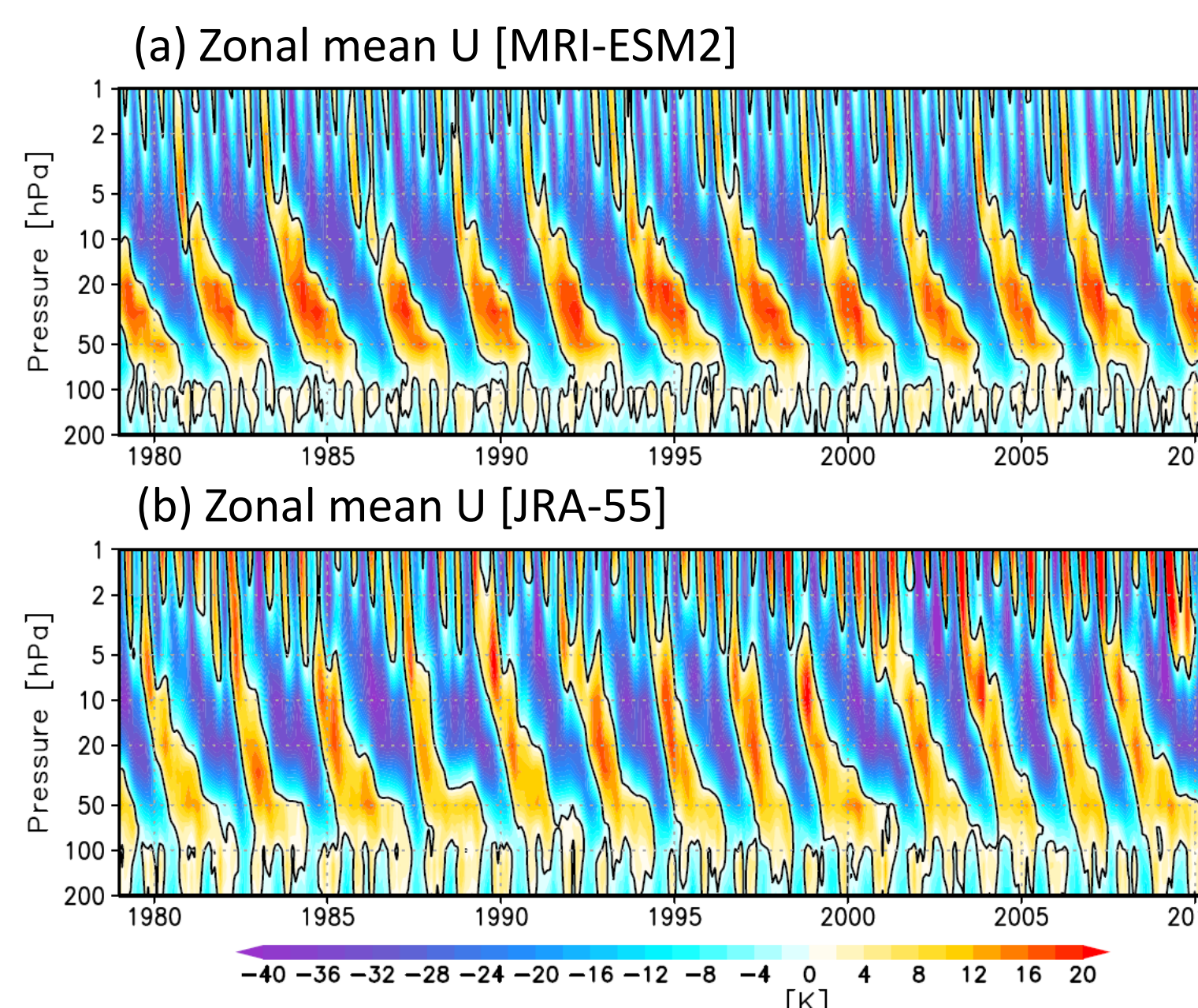
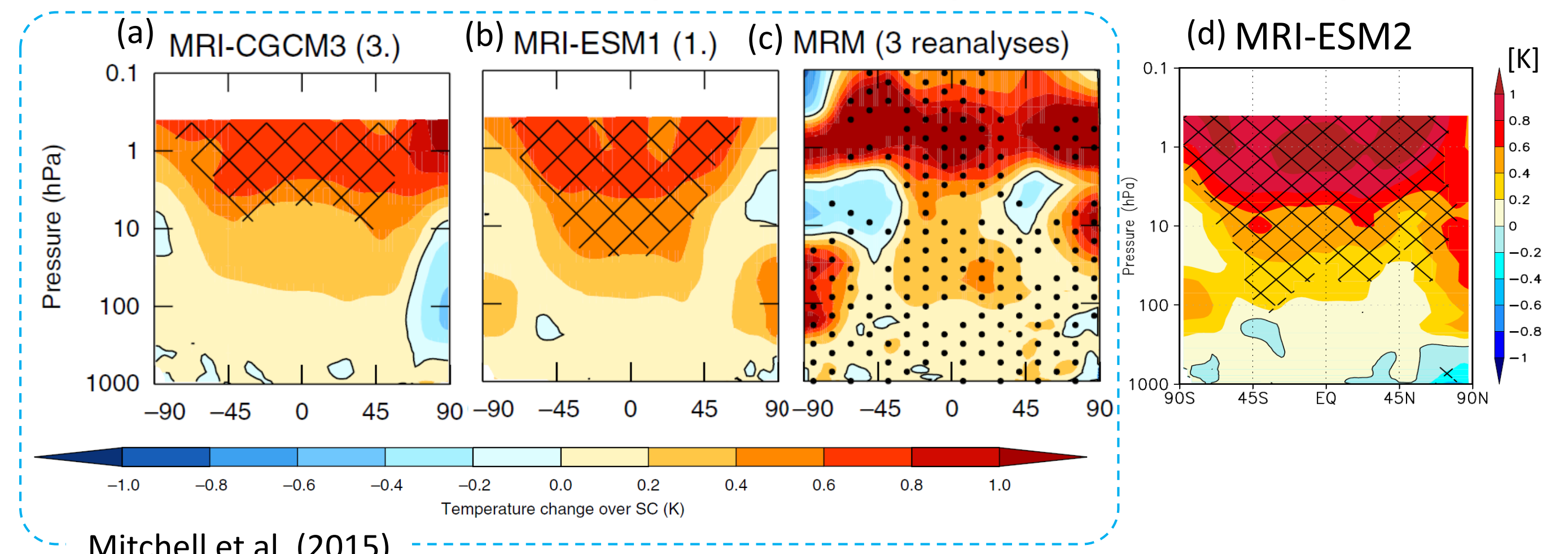


Fig. 6. Time series of zonal mean zonal wind averaged between 5°S and 5°N in (a) historical exp. of MRI-ESM2 (b) JRA-55

- Realistic QBO!
- Increase of vertical resolution and non-orographic gravity wave drag parameterization (Hines, 1997) contribute to drive QBO.
- Excessive amplitude at around 30 hPa.

Annual mean temperature response to solar cycle



Mitchell et al. (2015)

Multiple linear regression

$$y = ax_1 + bx_2 + cx_3 + dx_4 + ex_5 + fx_6 + \epsilon$$

y : Temperature
 a : Solar cycle (Total solar irradiance)
 b : Aerosol optical depth for volcanic H_2SO_4 at 550 nm
 c : QBO EOF1
 d : QBO EOF2
 e : ENSO (Niño 3.4)
 f : Green house gases (CO_2)

Fig. 7. Annual mean response of temperatures in (a) MRI-CGCM3 (b) MRI-ESM2 (c) Multi-reanalysis mean (d) MRI-ESM2 to solar variations derived from multiple linear regression. Calculation periods are (a,b,d) 1850-2005 and (c) 1979-2005. Hatches indicate 95% confidence intervals of statistical significance. Multi-reanalysis includes ERA-Interim, JRA-55, and MERRA. Figs 7a-c are quoted from Mitchell et al. (QJRM, 2015)

- Improve of temperature response to solar cycle especially in the upper stratosphere.
- Increase of vertical resolution and replacement of solar forcing may be important factor.

Zonal mean zonal wind [60°N, 10 hPa]

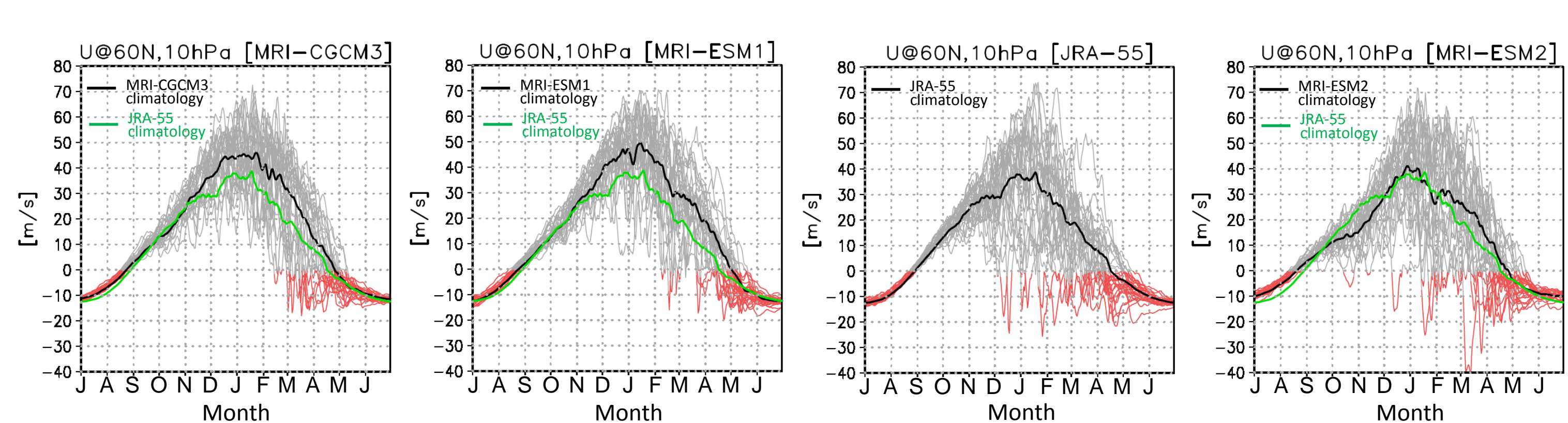
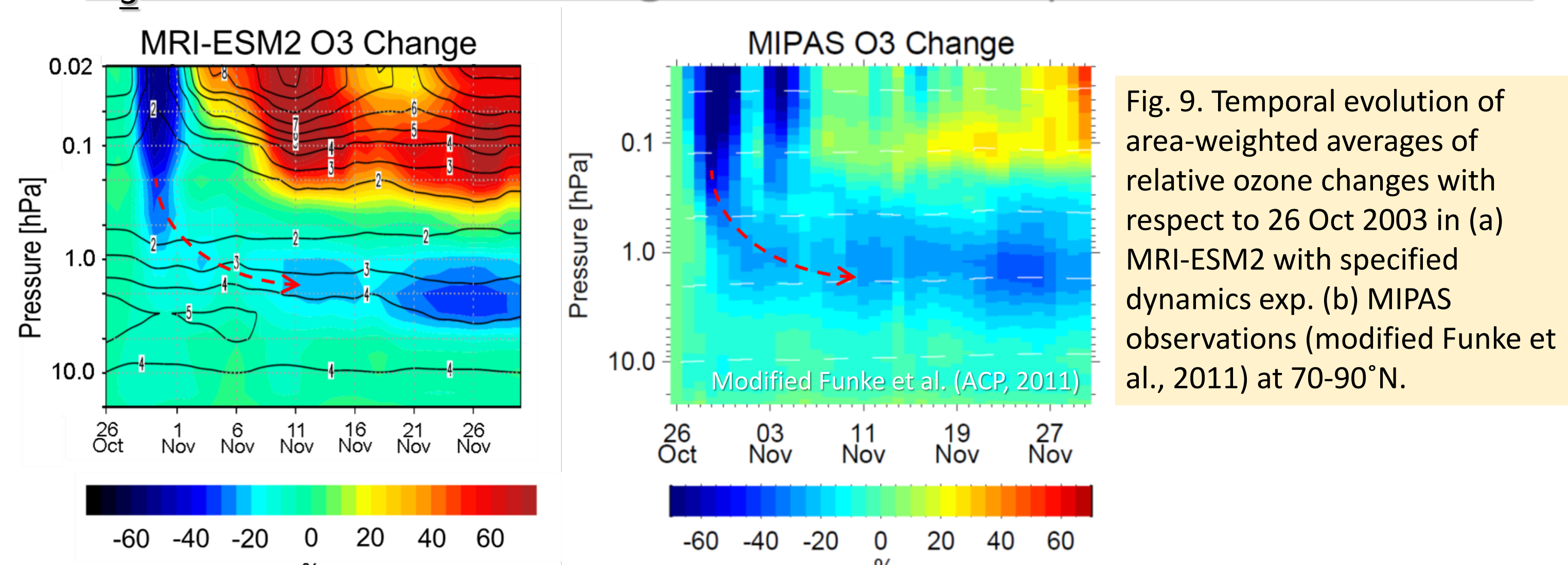


Fig. 8. Zonal mean zonal wind at 60°N and 10 hPa in (a) MRI-CGCM3 (b) MRI-ESM1 (c) JRA-55 (d) MRI-ESM2 for 1979-2005. Grey or red lines are zonal wind for each year, black lines are climatology, and green lines are climatology in JRA-55. Grey and red indicates positive and negative values, respectively.

- Improving SSW frequency
- Reducing strong wind bias in boreal winter
- Weak wind bias in November

O₃ reduction due to Energetic Particle Precipitation event in 2003



- MRI-ESM2 reproduces variation of O₃ during extreme solar proton (Halloween) event in 2003.
- Parameterization of NO_y production due to energetic particle precipitation (EPP) contributes to this change.